

1 ***In vitro* macronutrient digestibility and mineral**  
2 **bioaccessibility of lentil-based pasta: the influence of cellular**  
3 **intactness**

4 **Duijsens, D.<sup>a\*</sup>, Alfie Castillo A. I.<sup>a</sup>, Verkempinck, S.H.E.<sup>a</sup> Pälchen K<sup>a</sup>, Hendrickx, M.E.<sup>a</sup>,**  
5 **Grauwet, T.<sup>a\*\*</sup>**

6  
7 <sup>a</sup> Laboratory of Food Technology and Leuven Food Science and Nutrition Research Centre  
8 (LFoRCe), Department of Microbial and Molecular Systems (M2S), KU Leuven, Kasteelpark  
9 Arenberg 22, PB 2457, 3001, Leuven, Belgium

10  
11 **Author's email addresses:**

12 Duijsens, D.: [dorine.duijsens@kuleuven.be](mailto:dorine.duijsens@kuleuven.be)

13 Alfie Castillo A.I.: [aialfie1@gmail.com](mailto:aialfie1@gmail.com)

14 Verkempinck, S.H.E.: [sarah.verkempinck@kuleuven.be](mailto:sarah.verkempinck@kuleuven.be)

15 Pälchen, K.: [katharinapaelchen@outlook.de](mailto:katharinapaelchen@outlook.de)

16 Hendrickx, M.E.: [marceg.hendrickx@kuleuven.be](mailto:marceg.hendrickx@kuleuven.be)

17 Grauwet, T.: [tara.grauwet@kuleuven.be](mailto:tara.grauwet@kuleuven.be)

18 Journal: Food Chemistry

19 \* author to whom correspondence should be addressed during submission process:

20 [dorine.duijsens@kuleuven.be](mailto:dorine.duijsens@kuleuven.be)

21 +32 32 16 33 03 20

22 \*\* author to whom correspondence should be addressed post-publication:

23 [tara.grauwet@kuleuven.be](mailto:tara.grauwet@kuleuven.be)

24 +32 16 32 19 47

CONFIDENTIAL

25 **Abstract**

26 Recently, pulse ingredients with (partial) cellular intactness are put forward as promising  
27 innovative food ingredients with slowed macronutrient digestibility. This study compared cooking  
28 quality and nutrient (starch, protein, and mineral) digestibility/bioaccessibility of lentil-based pasta  
29 prepared from 100% raw-milled flour, and by substituting 30% of the formulation by isolated  
30 cotyledon cell powder or whole precooked powder. Formulation had little effect on cooking  
31 properties. Both amylolysis and proteolysis were significantly slowed by incorporating cellular  
32 ingredients: towards the end of simulated digestion, amylolysis was lowered by 16-25%, while  
33 differences in proteolysis became small. Cellular ingredient incorporation slightly decreased Zn  
34 and Mg but did not affect Ca and Fe bioaccessibility, overall yielding a low mineral  
35 bioaccessibility comparable to cooked whole pulses. To conclude, lentil-based pasta substituted  
36 with cellular ingredients showed improved nutritional properties (*i.e.*, high in digestible protein  
37 and slowed amylolysis), with perspectives for the development of different innovative foods with  
38 targeted nutritional properties.

39 **Key words**

40 Lentil noodles; nutrient bioencapsulation; INFOGEST; amylolysis; proteolysis; microstructure

41 **List of abbreviations**

42	DM	Dry matter
43	WM	Wet matter
44	RM	Raw-milled lentil flour
45	ICC	Isolated cotyledon cell powder

46	WL	Whole precooked lentil flour
47	100%RM	Pasta prepared from 100% raw-milled flour
48	30%ICC	Pasta prepared from 70% raw-milled flour and 30% ICC powder
49	30%WL	Pasta prepared from 70% raw-milled flour and 30% WL powder
50	PSD	Particle size distribution
51	DSC	Differential scanning calorimetry
52	SSF	Simulated salivary fluid
53	SGF	Simulated gastric fluid
54	SIF	Simulated intestinal fluid
55	ADR	Average daily requirement

CONFIDENTIAL

## 56 **1 Introduction**

57 A shift towards more plant-based diets seems inevitable for feeding the rising human population  
58 healthily and sustainably. Pulses are increasingly put forward as part of these diets as they are rich  
59 in (slowly) digestible starch, protein, fiber, minerals, and bioactive compounds (*e.g.*, phytates and  
60 polyphenols). While pulses are generally rich in minerals, the bioaccessibility and absorption of  
61 minerals are mostly low due to the presence of antinutrient chelators *e.g.*, phytic acid, pectin, and  
62 polyphenols (Duijsens et al., 2021). As pulses could be an important protein source in healthy and  
63 sustainable diets, their contribution to human mineral supply is important. Minerals play a crucial  
64 role in sustaining human health, with 1.5 to 2.0 billion people in all regions of the world suffering  
65 from one or multiple chronic mineral deficiencies (Galani, Orfila, & Gong, 2022). Poor  
66 bioaccessibility and bioavailability (often the case in plant-based foods) is considered an important  
67 cause of mineral deficiency, next to insufficient dietary intake and physiological condition of the  
68 consumer (*e.g.*, illness) (Platel & Srinivasan, 2016).

69 While pulses are a staple in several parts of the world, they have become underused in most of the  
70 western world due to sensory issues, their inconvenient long cooking times, and a lack of  
71 knowledge on how to prepare them (Henn et al., 2021). Incorporating pulse-based ingredients into  
72 staples may be a useful strategy to increase pulse consumption without drastically altering  
73 consumer dietary habits (Duijsens et al., 2021). In this regard, pasta and noodles are easy-to-  
74 prepare staples, highly consumed in several regions of the world. Alternative flour sources for  
75 pasta preparation (*e.g.*, pulses) are being explored with the aim of improving nutritional properties,  
76 such as more complete amino acid profiles and reduced starch digestibility (Garcia-Valle, Bello-  
77 Pérez, Agama-Acevedo, & Alvarez-Ramirez, 2021). Purely pulse-based pasta showed important  
78 nutritional potential compared to wheat-based pasta, *e.g.*, due to higher protein (up to around 30%

79 *versus* 13-14%, respectively) and fiber (around 7% *versus* 2%, respectively) contents (Laleg,  
80 Barron, Santé-Lhoutellier, Walrand, & Micard, 2016; Rosa-Sibakov et al., 2016), while exhibiting  
81 similar starch digestibilities (Petitot, Barron, Morel, & Micard, 2010; Rosa-Sibakov et al., 2016).  
82 Moreover, pulse-based pasta showed improved cooking quality (cooking loss and texture) and  
83 nutritional properties (high protein, fiber, and resistant starch) compared to gluten-free cereal pasta  
84 (Laleg, Cassan, Barron, Prabhasankar, & Micard, 2016). Interestingly, in 100% pulse-based pasta,  
85 starch is enveloped in a thick but weak protein network, formed by electrostatic forces and  
86 hydrogen bounds which mainly strengthen upon cooking (Laleg, Barron, et al., 2016).

87 In pulses, macronutrients are entrapped or bioencapsulated by a cell wall and intracellular (protein)  
88 matrix. Upon cooking, the gradual solubilization of pectin in the middle lamella causes the  
89 prominent tissue failure mode to shift from cell breakage to separation. As a consequence of  
90 cellular nutrient encapsulation, during digestion of cooked pulses, enzyme diffusion towards the  
91 substrate is hindered and the hydrolysis of entrapped starch and protein retarded (Duijsens et al.,  
92 2021; Gwala et al., 2019; Pälchen, Van Den Wouwer, et al., 2022; Zahir, Fogliano, & Capuano,  
93 2018). In contrast, pulse flours used in commercial applications such as pasta are manufactured by  
94 raw milling, mostly disrupting the microstructural complexity, rendering nutrients readily  
95 accessible to digestive enzymes. To exploit the inherent potential of the characteristic pulse  
96 microstructure, powders rich in intact cotyledon cells were produced from cooked pulses and  
97 incorporated into several foods with reduced *in vitro* and *in vivo* rates of amylolysis (Bajka et al.,  
98 2021). In this context, chickpea purees made up of isolated cotyledon cell powder showed a  
99 significantly increased satiety *in vivo*, compared to isocaloric chickpea puree without nutrient  
100 bioencapsulation (Pälchen, Bredie, et al., 2022).

101 Recently, the authors of this work studied the effect of manufacturing conditions on the digestion  
102 kinetics of lentil powders with (partial) cellular intactness, *i.e.*, isolated cotyledon cell powder  
103 (ICC) and whole precooked lentil powder (WL) (Duijsens, Pälchen, De Coster, et al., 2022).  
104 However, knowledge on the technofunctional and digestion properties of these innovative powders  
105 upon incorporation into highly structured foods such as pasta was still missing. Therefore, in this  
106 follow-up work, the effect of partially (30%) incorporating powders with cellular intactness into a  
107 purely lentil-based pasta formulation was studied on the pasta cooking properties. Moreover, the  
108 effect on *in vitro* amylolysis and proteolysis kinetics of these pastas was evaluated. To assess the  
109 potential of pulse-based pasta as a mineral supplier, magnesium, calcium, iron, and zinc  
110 bioaccessibility values were studied as examples of major and trace minerals.

## 111 **2 Materials and Methods**

### 112 **2.1 Materials**

113 Green (Dupuy) lentils (*L. culinaris*) were grown and harvested in Canada (August 2019) and  
114 donated by Casibbeans (Melsele, Belgium). The material (<10% moisture) was sorted and cleaned  
115 from foreign material, followed by storage below the glass transition temperature to ensure  
116 stability (-40 °C). Chemical reagents and enzymes were purchased from Merck KGaA (Germany),  
117 except for the Total Starch Kit (Megazyme, Bray, Ireland), KCl, MgCl<sub>2</sub>(H<sub>2</sub>O)<sub>6</sub>, NaOH, sodium  
118 potassium tartrate (Acros Organics, Geel, Belgium), NaHCO<sub>3</sub>, NaCl, KH<sub>2</sub>PO<sub>4</sub> (VWR, Leuven,  
119 Belgium).

### 120 **2.2 Lentil ingredient preparation**

121 Lentil flours with different microstructures were prepared as previously reported (Duijsens,  
122 Pälchen, De Coster, et al., 2022). Briefly, raw lentils were milled to pass through a 500 µm sieve  
123 mesh (Cyclotec1093 sample mill, FOSS, Sweden) (*raw-milled flour*). Additionally, lentils were

124 soaked (1:10 w/v, 25 °C, 16 h), cooked (1:10 w/v, 95 °C, 15 min), mixed with demineralized water  
125 (1:1 w/v), and homogenized (2 min, 3000 rpm) (IKA® T25 Ultra-Turrax, Janke and Kunkel,  
126 Germany). From these cooked lentils, two distinct powders containing structurally intact cells were  
127 prepared. Firstly, *isolated cotyledon cell flour (ICC)* was prepared by isolating cotyledon cells  
128 from the slurry by wet-sieving (amplitude 2.5 mm, 4 min) (AS200, Retsch, Germany), and  
129 lyophilizing the individual cotyledon cell fraction (40-125 µm) (Alpha 1-4 LSCplus, Martin Christ,  
130 Germany). Secondly, *whole precooked lentil flour (WL)* was prepared by lyophilizing the cooked  
131 lentil slurry as such. The freeze-dried powder was sieved (500 µm mesh), after which the (seed  
132 coat) fraction >500 µm was blended (IKA Labortechnik-A10, Germany), re-sieved, and mixed  
133 again with the other fraction (<500 µm) to obtain a homogenous powder.

### 134 **2.3 Lentil pasta preparation**

135 To produce pasta, free starch and protein are necessary in the flour to form a continuous phase  
136 (Laleg, Cassan, et al., 2016). Therefore, a ratio of substitution with the (partially) cellular  
137 ingredients was chosen at which it was hypothesized that (i) there would be a limited effect on the  
138 possibility to form a continuous phase, a dough with an acceptable consistency, and subsequently  
139 a pasta with acceptable cooking properties (meaning sufficient free starch and protein were  
140 present), and (ii) enough intact cellular material would be present to significantly affect starch  
141 digestion kinetics. Based on these requirements and previous results for partial substitution of  
142 wheat-based food formulations by cellular ingredients (Bajka et al., 2021), a ratio of 70:30 (w/w,  
143 wet basis) raw-milled flour with ICC and WL powders was selected for this work. It was  
144 hypothesized that, applying this ratio, the formed network, mainly consisting of free proteins,  
145 would entrap free starch granules, as well as cotyledon cells (provided by ICC and WL), finally  
146 delivering a pasta with acceptable cooking properties but significantly slowed starch digestion.



147 From here on, pasta samples made from pure raw-milled flour, 30% ICC powder, and 30% WL  
148 powder will be referred to as 100%RM, 30%ICC, and 30%WL, respectively.

### 149 *2.3.1 Dough preparation*

150 The moisture required for dough preparation was determined for each flour mixture using a  
151 farinograph-E (Brabender, Germany) with a 50 g mixing bowl (Sigma mixer S 50, Brabender,  
152 Germany). Briefly, 43 g of flour (dry matter) was weighed into a temperature-controlled mixer  
153 with continuously rotating blades (63 rpm). Upon water addition, the resistance of the formed  
154 dough to mixing was measured. Different moisture additions were tested iteratively, targeting a  
155 standard dough consistency of 500 B.U. (Patel & Chakrabarti-Bell, 2013). For each pasta, 300 g  
156 of flour (mixture) was kneaded (10 min, 100 rpm) in the mixing bowl of a Thermomix TM6 mixer  
157 (Vorwerk, Germany). The predetermined amount of water (reported in **Table 1**) was gradually  
158 added during the first seconds of kneading. The obtained dough was rested in a plastic bag at 4 °C  
159 for 30 min.

### 160 *2.3.2 Pasta preparation*

161 Pasta preparation was based on the procedures of Gallegos-Infante et al. (2010) and Giuberti,  
162 Gallo, Cerioli, Fortunati, & Masoero (2015). The kneaded dough was divided into small balls  
163 (approximately 30 g). Each dough ball was sheeted through the rollers of a manual pasta machine  
164 (Atlas 150, Marcato, Italy), twice per setting (0, 1, and 2 of 4.8, 3.8, and 3.3 mm, respectively).  
165 The laminated dough was cut into strips using a spaghetti chitarra attachment (Atlas 50, Marcato,  
166 Italy) (diameter 2 mm, length approximately 10 cm). The pasta was dried on trays using natural  
167 air convection (16 h, 25 °C) and then stored in glass jars in a dry and dark environment until  
168 utilization.

169 2.3.3 Determination of cooking properties and cooking quality

170 *Optimal cooking time (OCT)*. For each pasta type, the optimal cooking time was determined  
171 following the approved 66-50 method (AACC 2000) (Laleg, Cassan, et al., 2016; Petitot & Micard,  
172 2010). Briefly, the minimum cooking time was determined as the cooking time at which the starchy  
173 core disappeared (qualitatively) upon squeezing between two glass plates. Then, the OCT was  
174 determined as the minimal cooking time plus one minute (**Table 1**). In view of the evaluation of  
175 starch digestibility, DSC analysis confirmed complete starch gelatinization upon cooking for the  
176 OCT (*data not shown*).

177 *Cooking loss*. For each pasta type, a duplicate analysis of cooking loss was carried out by cooking  
178 15 g pasta in 250 mL demineralized water. Cooking losses were calculated using Eq.1 (Laleg,  
179 Barron, et al., 2016). Additionally, starch and protein losses upon cooking were determined,  
180 considering the respective content in the cooked and uncooked pasta samples.

181 
$$\text{Cooking loss (\%, dm)} = \frac{\text{cooked pasta (g, DM)} - \text{uncooked pasta (g, DM)}}{\text{uncooked pasta (g, DM)}} \times 100\% \quad \text{Eq.1}$$

182 *Water uptake*. The water uptake was determined gravimetrically, upon cooking pasta in duplicate  
183 as stated above, according to Eq.2.

184 
$$\text{Water uptake (\%)} = \frac{\text{cooked pasta (g, WM)} - \text{uncooked pasta (g, WM)}}{\text{uncooked pasta (g, WM)}} \quad \text{Eq.2}$$

185 **2.4 Characterization of produced spaghetti**

186 2.4.1 *Microscopy*

187 Cooked pasta samples were analyzed using an Olympus BX-51 light microscope (Olympus,  
188 Optical Co. Ltd, Tokyo, Japan) with 10x objectives and cellSense Standard® software. A thin slice

189 (about 1 mm) of pasta was squeezed between a microscope slide and a cover glass to visualize the  
190 cooked samples.

#### 191 2.4.2 Proximate analysis

192 The composition of each produced (uncooked and cooked) pasta was determined. Starch content  
193 was determined in duplicate (total starch kit, AA/AMG, Megazyme Inc. Bray, Ireland). Nitrogen  
194 content was analyzed in duplicate by automated Dumas analysis (CE instrument, Thermofischer  
195 Scientific, Waltham, USA), applying a 5.4 conversion factor to calculate the crude protein content  
196 (De Almeida Costa, Da Silva Queiroz-Monici, Pissini Machado Reis, & De Oliveira, 2006). The  
197 moisture content was determined in duplicate as the mass difference upon oven drying (Jouan,  
198 France) (100 °C, 24 h). The lipid content was determined according to Janssen et al. (2018), in  
199 triplicate. The ash content was determined in triplicate as the weight loss upon complete  
200 incineration (muffle furnace, 550 °C, 20 h). Hereafter, the Mg, Ca, Fe, and Zn contents were  
201 determined by inductively coupled plasma optical emission spectroscopy (ICP-OES) (Gwala et  
202 al., 2020). To do so, the obtained ashes were dissolved in 10 mL MilliQ-water containing 1% nitric  
203 acid solution and stored overnight (24 h, 25 °C). Subsequently, the solutions were filtered using a  
204 0.45 µm membrane filter (Chromaphil® A-45/25, Macherey-Nagel, Germany). Mineral analysis  
205 was carried out by ICP-OES (ICAP 7000 series, Thermo Fisher Scientific), radially at 285 and 318  
206 nm for Mg and Ca, and axially at 238 and 206 nm for Fe and Zn. Before each run and after 20  
207 samples, a calibration using SPS-SW2 was performed. Certified reference materials (BCR-129  
208 and BCR-679, Joint Research Centre, European Commission) were analyzed to ensure accuracy  
209 of the quantification (recoveries in *Supplementary material 1*). Finally, the fiber-rich residue  
210 (containing high amounts of fiber and sugars among which undigestible galacto-oligosaccharides)  
211 was calculated by difference from the starch, protein, moisture, lipid, and ash content.

## 212 **2.5 *In vitro* digestion of pasta samples**

213 *In vitro* digestion of lentil pastas with different microstructural properties was executed following  
214 the static INFOGEST protocol (Brodkorb et al., 2019). To study the digestion process as a function  
215 of time, digestion was performed in independent, individual tubes (5 gastric and 13 small intestinal  
216 time points) for each considered sample. Enzyme blanks (*i.e.*, no sample but all reagents) were  
217 prepared for the gastric and small intestinal phase.

218 Immediately before digestion, lentil pasta was cooked (OCT), rinsed with demineralized water to  
219 stop the cooking process, and drained for 2 min. To mimic the particle size distribution upon  
220 mastication of spaghetti (ranging 5 – 30 mm with an average of 10 mm according to Hoebler et al.  
221 (1998)), cooked samples were cut into pieces of about 10 mm with a knife, as previously applied  
222 by Freitas & Le Feunteun (2019). 1.25 g of sample were weighed into each reaction tube and the  
223 oral, gastric, and small intestinal phases were simulated exactly as reported earlier (Duijsens,  
224 Pälchen, De Coster, et al., 2022). During simulation of the different digestion phases, conditions  
225 (pH, temperature, and enzyme activity) were kept constant, ensuring that time-dependent enzyme-  
226 substrate interactions (and metabolite release) can be studied under physiologically relevant  
227 conditions. Samples were taken at predetermined time points followed by thermal enzyme  
228 inactivation (5 min, 98 °C). Digests were centrifuged (2000 g, 5 min, 25 °C) and separated into a  
229 soluble supernatant containing bioaccessible nutrients, and an insoluble pellet. Both fractions were  
230 snap-frozen using liquid nitrogen and stored until analysis (-40 °C).

### 231 **2.5.1 *Determination of digested starch***

232 Amylolysis was quantified in the small intestinal phase since amylase was only incorporated at  
233 this stage of the simulation. The extent of starch digestion (%) was evaluated using the  
234 dinitrosalicylic (DNS) method, exactly as described earlier (Duijsens, Pälchen, De Coster, et al.,

235 2022). The concentration of reducing sugars in each sample was calculated using a maltose  
236 calibration curve, and the maltose concentration was converted to starch using a conversion factor  
237 of 0.95 (Eq.3).

$$238 \text{ Digested starch (\%)} = \frac{\text{maltose equivalents} \times 0.95}{\text{total starch content}} \times 100 \quad \text{Eq.3.}$$

239 The DNS method quantifies reducing groups, using maltose as a reference. Starch hydrolysis by  
240 (pancreatic) amylase mostly yields maltose and maltotriose, but other products such as glucose  
241 can be formed too, possibly causing an overestimation in the obtained amylolysis extent (Warren,  
242 Zhang, Waltzer, Gidley, & Dhital, 2015). The chromatographic quantification of different starch  
243 hydrolysis products can be a strategy to avoid such overestimations. Comparison of DNS with  
244 HPAEC-PAD revealed an overestimation of final amylolysis extents determined by DNS of  
245 around 10% (Gwala et al., 2019), while amylolysis kinetics generally followed similar patterns. In  
246 this regard, *in vitro* digestion assays are suited to deliver insight into digestion patterns and rates  
247 and allow the comparison of samples under fixed conditions (*e.g.*, enzymatic activity) (Warren et  
248 al., 2015). However, these simulations are less suited for the predictions of exact amylolysis  
249 extents *in vivo* (Duijsens, Pälchen, Guevara-Zambrano, et al., 2022; Warren et al., 2015).  
250 Therefore, the DNS method is a suitable, widely applied, and rapid method for the analysis and  
251 comparison of amylolysis kinetics and patterns, even though it does not distinguish between  
252 different formed metabolites.

### 253 2.5.2 Determination of digested protein

254 Protein digestion was evaluated using the spectrophotometric o-phthalaldehyde (OPA) assay,  
255 quantifying  $\alpha$ -amino groups released upon proteolysis, according to Zahir et al. (2018), as  
256 previously described in detail (Duijsens, Pälchen, De Coster, et al., 2022).

257 To quantify the *total α-amino groups present in the undigested sample* ( $NH_{2total}$ ), 5 mg of sample  
 258 was hydrolyzed in 1 mL 6 N HCl (24 h, 110 °C) in duplicate. Afterwards, the acid was removed  
 259 by rotary evaporation (Hei-Vap Core, Heidolph, Germany), samples were diluted in 5 mL MilliQ,  
 260 and filtered (pore size 0.25 μm). Proteolysis was then quantified in two ways. The *readily*  
 261 *bioaccessible fraction* ( $NH_{2TCA}$ ) was quantified by precipitating large peptides from the digestive  
 262 supernatant (through addition of 3.2% TCA) (Zahir et al., 2018). After centrifugation (10 000 g,  
 263 25 °C, 30 min) (Microfuge 22R, Beckman Coulter, US), the resulting supernatant was filtered.  
 264 The small peptides in the TCA-treated supernatant were considered to be absorbable at intestinal  
 265 brush border. In parallel, the *hydrolyzed readily bioaccessible fraction* ( $NH_{2TCA,hydro}$ ) was  
 266 evaluated.  $NH_{2TCA,hydro}$  represents the same fraction as  $NH_{2TCA}$ , but expressed in terms of amino  
 267 acid constituents and thus more easily relatable to the total protein amount (*i.e.*, α-amino groups)  
 268 in the undigested sample ( $NH_{2total}$ ). For this, the TCA-soluble peptides were hydrolyzed in 6 N  
 269 HCl (16 h, 110 °C), the acid was evaporated, the samples were redissolved, and filtered.  
 270 For each set of analyses, OPA reagent was (freshly) prepared according to Zahir et al. (2018).  
 271 Detected amino groups were converted into serine equivalents using an L-serine standard curve  
 272 (12.5-100 mg/mL). The analysis was carried out as stated earlier (Duijsens, Pälchen, De Coster, et  
 273 al., 2022), and the extent of proteolysis was calculated as indicated in equations 4 and 5.

$$274 \text{ readily bioaccessible protein} = \frac{NH_{2TCA} - NH_{2initial}}{NH_{2total}} * 100\% \quad \text{Eq.4}$$

$$275 \text{ hydrolyzed readily bioaccessible protein} = \frac{NH_{2TCA,hydro} - NH_{2initial}}{NH_{2total}} * 100\% \quad \text{Eq.5}$$

### 276 2.5.3 Determination of mineral bioaccessibility

277 The mineral bioaccessibility was determined (Eq.6) according to Gwala, Kyomugasho et al.  
 278 (2020), from the digestive supernatants (see *Section 2.4.2*). Mineral bioaccessibility was evaluated

279 at 5 small intestinal time points (0,10, 90, 120, and 150 minutes). Since the data revealed no effect  
280 of small intestinal digestion time on mineral bioaccessibility (in accordance with literature (Gwala  
281 et al., 2020; Rousseau, Pallares Pallares, Vancoillie, Hendrickx, & Grauwet, 2020)), an average  
282 mineral bioaccessibility was calculated over the considered digestion times.

$$283 \text{ Mineral bioaccessibility} = \frac{\text{mineral conc. in digest} - \text{mineral conc. in blank}}{\text{mineral conc. in the sample}} \times 100\% \quad \text{Eq.6}$$

## 284 **2.6 Kinetic modelling and statistical analysis**

285 As elaborated earlier, macronutrient digestion kinetics were studied by determining digestion  
286 products in each of the produced digests. Each of these digests represents an independent,  
287 consecutive measurement of the same digestive behavior as recently reviewed (Duijsens, Pälchen,  
288 Guevara-Zambrano, et al., 2022). Macronutrient digestibility of different samples was evaluated  
289 by integrating the data of all kinetic points by mathematical modelling, and subsequently  
290 comparing the obtained curves and estimated parameters.

291 To integrate the kinetic data of macronutrient digestion during the small intestinal phase, a first  
292 order fractional conversion model was applied (Gwala et al., 2019), shown in equation 7, with  $C$   
293 the extent (%) of macronutrient hydrolysis at a certain digestion time.  $C_0$  was defined as the  
294 hydrolysis extent at the beginning of the small intestinal phase ( $t=0$ ) (and thus the end of the gastric  
295 phase). The final hydrolysis extent  $C_f$  (%) and the rate constant  $k$  ( $\text{min}^{-1}$ ) were simultaneously  
296 estimated by nonlinear regression (SAS version 9.4, SAS Institute, Inc., Cary, NC, USA). The fit  
297 of the modelled curves was assessed by calculating  $R^2_{\text{adj}}$  and drafting residual and parity plots.  
298 Significant differences between the parameters were evaluated based on 95% confidence intervals.  
299 For the case of starch digestion, since no salivary amylase was incorporated into the simulated oral  
300 phase, it was assumed no orogastric amylolysis took place ( $C_0=0$ ). Moreover, the initial reaction

301 rate ( $v_{\text{initial}}$ ) was calculated from the slope of the tangent line to the modelled amylolysis curve at  
302 time 0.

$$303 \quad C(t) = C_f + (C_0 - C_f) * e^{-k*t} \quad \text{Eq.7}$$

304 To assess significant differences between mean compositions and mineral bioaccessibilities, one-  
305 way ANOVA and Tukey's HSD tests ( $p < 0.05$ ) were performed (JMP16, SAS Institute Inc., Cary,  
306 NC, USA), while 95% confidence intervals were used for fiber-rich residues.

### 307 **3 Results and discussion**

#### 308 **3.1 Cooking properties and quality of pasta**

309 The cooking properties of the pasta samples were summarized in **Table 1**.

310 The **moisture addition** required to form the 100%RM dough (49%) was similar to the amount  
311 reported by for raw-milled fava bean dough (42%) (Rosa-Sibakov et al., 2016). A higher moisture  
312 addition (70-74%) was observed for the 30%ICC and 30%WL doughs. Plausibly, this could be  
313 caused by the (i) higher water holding capacity of flours with cellular intactness (Bajka et al., 2021)  
314 and (ii) lower water absorption of native semi-crystalline starch (present in raw-milled flour) as  
315 compared to pre-gelatinized starch (present in precooked ICC and WL powders) (Noordraven,  
316 Bernaerts, Mommens, Hendrickx, & Van Loey, 2021).

317 A slightly longer **OCT** was observed for the 100%RM spaghetti (15 min) compared to the other  
318 samples (12 min). In literature, OCT has been related to the (ungelatinized) starch content of the  
319 pasta. Indeed, 30%ICC and 30%WL were partially composed of a thermally pretreated ingredient  
320 in which starch was pregelatinized and protein denatured, possibly explaining their shorter OCT.

321 **Dry matter losses** (10-16%) observed for the three pasta samples are similar to values reported  
322 earlier for purely pulse-based pasta (e.g. 13% for lentil (Laleg, Cassan, et al., 2016) and 11% for



323 fava bean pasta (Rosa-Sibakov et al., 2016)). In contrast, cooking losses of 6 to 8% dry matter  
324 were reported for wheat semolina pasta, while a value of 9% was reported for wheat-based pasta  
325 partially substituted with fava bean flour (Laleg, Barron, et al., 2016; Rosa-Sibakov et al., 2016).  
326 A higher cooking loss in pulse-based pasta compared to wheat-based formulations (partially  
327 substituted with pulse flour or not) was attributed to a weaker, more water-soluble protein network  
328 formed upon cooking of pulse-based pasta compared to the covalently bound wheat gluten network  
329 100. In the context of wheat-based pasta, fiber was previously reported to physically interfere with  
330 the formation of a continuous gluten network in pasta (Dodi et al., 2021). Plausibly, fiber (present  
331 in higher amounts in RM and WL powders due to the seed coat present) could disrupt the  
332 continuity of the non covalently bound pulse protein network in the pasta samples studied here as  
333 well, hereby increasing cooking loss.

334 The 30%ICC pasta presented lower DM losses upon cooking than the two other samples. Due to  
335 the composition of the ICC powder (100% isolated cotyledon cells), it is hypothesized that the  
336 higher degree of nutrient bioencapsulation may have contributed to the limited leaching in the  
337 30%ICC pasta compared to the other samples. Moreover, the 30%ICC flour mixture contained  
338 relatively fewer large seed coat particles (such as seed coat material) compared to the other two  
339 pasta samples. Next to differences in microstructure (*i.e.*, degree of nutrient bioencapsulation) and  
340 contribution of seed coat particles, the higher dry matter loss of the 100%RM compared to the  
341 other two samples may be due to the longer OCT applied for this sample as well. However, this  
342 research aimed to compare pasta quality and digestion attributes of pasta cooked to an equivalent  
343 palatable point (requiring different OCTs) at which starch gelatinization was complete.

344 In terms of **water uptake** (approximately 290%), the studied pastas triplicated in weight upon  
345 cooking. Similar water uptake was reported for a wheat-based pasta enriched with raw-milled

346 common bean flour (Gallegos-Infante et al., 2010), produced manually similarly to the pasta in  
347 this work. In contrast, water absorption of 165% was reported for a 100% raw-milled lentil flour  
348 pasta (Laleg, Cassan, et al., 2016), and similar values were found for other wheat-based pastas  
349 partially enriched with pulse flour (Laleg, Barron, et al., 2016; Petitot & Micard, 2010), both  
350 prepared by extrusion. Therefore, it is expected that variations in water uptake of pasta samples  
351 strongly depend on the manufacturing method and final dimensions of the pasta, rather than the  
352 cellular integrity of the employed flour type.

### 353 **3.2 Microstructure of cooked pasta**

354 **Figure 1** shows representative micrographs of the microstructure of the (cooked) pasta before and  
355 after 90 min of small intestinal digestion. These images confirm the (at least partial) persistence of  
356 intact cotyledon cells, during dough handling, pasta manufacturing, drying, cooking, as well as  
357 simulated digestion.

358 Each of the produced pastas was composed of a continuous phase of free protein and starch  
359 provided by the raw-milled flour. While the raw-milled flour consisted of small fractionated  
360 material (among which free starch granules and protein bodies) and tissue fragments (such as cell  
361 clusters and seed coat particles), the pure ICC powder was composed of 100% individual cells  
362 physically entrapping macronutrients, and the pure WL powder consisted of approximately 63%  
363 of individual cells (40-300  $\mu\text{m}$ ) next to cell clusters, seed coat particles etc. (Duijsens, Pälchen, De  
364 Coster, et al., 2022). From the previously reported particle size distributions (PSDs) of the  
365 respective powders, the fraction of individual cells in the flour mixtures could be determined,  
366 indicating the possible incidence of cells in the final pasta to be around 30% in the 30%ICC  
367 mixture, and around 20% in the 30%WL flour mix. This was confirmed via laser scattering and  
368 microscopy (*data in Supplementary material 2*).

### 369 3.3 Composition of uncooked and cooked pasta

370 The chemical composition of the (uncooked and cooked) pasta samples is summarized in **Table**  
371 **2**. As can be seen from **Table 2**, the partial (30%) substitution of raw-milled whole lentil flour  
372 with a (partly) cellular ingredient slightly increases the protein and starch content. This is explained  
373 by the slightly higher starch and protein content in the ICC and WL flours, compared to the raw-  
374 milled one (Duijsens, Pälchen, De Coster, et al., 2022). The protein content and fiber-rich fraction  
375 of all pasta types produced here was remarkably higher as compared to wheat-based pasta (13-  
376 14% and 2.4%, respectively) (Laleg, Barron, et al., 2016; Rosa-Sibakov et al., 2016).

377 The fiber-rich residue and ash (mineral) content of 100%RM was slightly higher as compared to  
378 the 30%WL and 30%ICC pasta, due to partial replacement of the whole, raw-milled lentil  
379 ingredient by a precooked ingredient. Upon cooking, the ash content decreased due to mineral  
380 leaching. In more detail, **Figure 2A** shows the Fe, Zn, Mg, and Ca contents of the cooked and  
381 uncooked pasta samples. The mineral contents determined for the uncooked raw-milled pasta are  
382 in accordance with previously reported values in raw green lentils (Suliburska & Krejpcio, 2014).

383 For each of the considered pasta types, the Fe content did not significantly decrease upon cooking,  
384 similarly as during cooking of Bambara groundnuts and common beans (Gwala et al., 2020;  
385 Rousseau, Celus, et al., 2020). In pulses, non-ferritin Fe is expected to preferentially complex with  
386 phytates, minimizing leaching during cooking (Gwala et al., 2020; Moore et al., 2018). In contrast,  
387 the Mg and Zn content of the 100%RM significantly decreased upon cooking. Due to limited  
388 interactions with chelators, Mg ions leach more easily compared to other minerals as reviewed  
389 earlier (Duijsens et al., 2021). No significant decrease in Ca content was observed upon pasta  
390 cooking, in contrast with the small but significant decrease in Ca content upon cooking of Bambara  
391 groundnuts and common beans (Gwala et al., 2020; Rousseau, Celus, et al., 2020). Seed coat

392 particles present in the pulse flour are rich in fiber (see **Table 2**), oxalic acid, and polyphenols  
393 among others, which may have a protective effect against Ca leaching (Lombardi-Boccia et al.,  
394 1998).

### 395 **3.4 Starch hydrolysis upon *in vitro* digestion of pasta**

396 Starch hydrolysis kinetics upon *in vitro* small intestinal digestion of lentil pasta are shown in  
397 **Figure 3A**. All studied pastas first showed a period of increasing amylolysis, reaching a plateau  
398 upon long digestion times. The data were therefore modelled using the fractional conversion model  
399 (Eq. 7), with the estimated kinetic parameters summarized in **Table 3**. The fraction of starch which  
400 remains undigested upon 120 min of small intestinal digestion has been defined as resistant starch.  
401 Moreover, the extent of starch hydrolysis at 90 minutes of small intestinal digestion was reported  
402 to correlate to *in vivo* GI and can be a useful measure of starch digestibility (Edwards, Cochetel,  
403 Setterfield, Perez-Moral, & Warren, 2019). Therefore, next to the estimated final level of digestion  
404 ( $C_f$ ),  $C_{120}$  and  $C_{90}$  were compared among the studied samples.

405 Amylolysis in 100%RM occurred faster and, after 120 min of *in vitro* small intestinal digestion, to  
406 a higher extent (103%) compared to 30%WL (83%) and 30%ICC (72%) pasta, quantitatively  
407 supported by the significant differences in the kinetic parameters  $k$ ,  $v_{\text{initial}}$ , and  $C_{120}$  in **Table 3**.  
408 These results indicate that incorporating ingredients with cellular intactness (ICC and WL) into a  
409 pulse-based pasta could significantly reduce the rate and extent of starch hydrolysis, highlighting  
410 their potential to delay starch hydrolysis in such applications.

411 Amylolysis was slower in the 30%ICC compared to the 30%WL, which could be attributed to the  
412 differences in PSD and relative amounts of individual cells incorporated (see *Section 3.2*). The  
413 flour mixture for 30%ICC contained ~30% individual cells, compared to ~20% for the 30%WL  
414 pasta (*section 3.3*). The difference between ICC and WL powder composition was not limited to

415 the cellular fraction, as WL also contained seed coat particles (*i.e.*, fiber) (Duijsens, Pälchen, De  
416 Coster, et al., 2022). In general, a higher pulse fiber content has been linked to retarded amylolysis  
417 explained by non-specific interactions with amylases (Dhital, Gidley, & Warren, 2015). However,  
418 the addition of fiber in wheat-based pasta has been shown to disrupt the continuity of the protein  
419 matrix, rendering starch granules more susceptible to enzymatic degradation, increasing starch  
420 digestion kinetics by 15% (Dodi et al., 2021). While the higher fiber content of 30%WL and  
421 100%RM may have caused additional disruption of the continuous protein phase, its effect on  
422 amylolysis kinetics could (partially) be counteracted by the presence of bioencapsulated starch.

423 Clearly, starch hydrolysis was fastest for the 100%RM, reaching about 53% of amylolysis within  
424 the first 20 minutes of small intestinal digestion. Oppositely, the RM flour (evaluated in a heat-  
425 treated suspension) reached about 80% of starch digestion during the first 20 min of the small  
426 intestinal simulation (Duijsens, Pälchen, De Coster, et al., 2022). In contrast to the suspended  
427 system, pasta consists of a densely packed protein network surrounding starch, decreasing its  
428 accessibility for digestive enzymes. These findings indicate that the pasta structure was the major  
429 rate-determining physical barrier hindering amylolysis. Subsequently, by incorporating  
430 bioencapsulated starch (*i.e.*, 30%ICC and 30%WL), amylolysis can be slowed down further. These  
431 results confirmed once more to what extent nutrient digestibility can be influenced by both micro-  
432 and macro- structural properties of the food in which they are incorporated, highlighting the need  
433 for digestion studies for specific food applications.

434 In the available literature, a similar extent of 99% amylolysis upon 120 min of small intestinal  
435 digestion was reported for an extruded, dehulled raw-milled lentil pasta (Laleg, Cassan, et al.,  
436 2016), while around 75% was reported for a raw-milled chickpea macaroni (Garcia-Valle et al.,  
437 2021). Logically, next to nutrient bioencapsulation, differences in exact digestion kinetics among

438 samples can be caused by differences in pasta size, shape, thickness, and preparation technique  
439 (extrusion, drying temperature) (Petitot et al., 2009), determining the accessibility of the starch to  
440 amylases. However, these studies applied *in vitro* digestion protocols different from INFOGEST,  
441 rendering comparison difficult. Therefore, a commercial extruded (non-whole meal) wheat-based  
442 reference spaghetti was evaluated using the INFOGEST protocol (*data in Supplementary material*  
443 3). The wheat-based pasta exhibited a significantly slower starch hydrolysis ( $v_{\text{initial}}$ ) compared to  
444 the 100%RM pasta (approximately 80% after 90 minutes) while reaching a similar final level  
445 (approximately 100%), explained by both the presence of a covalently bound gluten network and  
446 the absence of a hull fraction. Generally, amylolysis of the commercial wheat-based pasta followed  
447 a similar course to the 30% WL, while amylolysis of 30%ICC was significantly (s)lower (in terms  
448 of  $v_{\text{initial}}$  and extent for each digestion time).

### 449 **3.5 Protein hydrolysis upon *in vitro* digestion of pasta**

450 The formation of bioaccessible protein upon digestion of cooked pasta made of lentil flour mixes  
451 with different degrees of cellular intactness is shown in **Figure 3B**.

452 At the end of the gastric phase, the amount of bioaccessible protein ( $\text{NH}_2\text{TCA}$ ) varied between 8  
453 and 12% compared to around 5% for a commercial wheat-based spaghetti (*data in Supplementary*  
454 *material 3*). Petitot et al. (2009) reported 3-8% gastric proteolysis for wheat semolina pasta, while  
455 Laleg, Barron et al. (2016) found that during 30 min of *in vitro* (pepsin) proteolysis, only 4% of  
456 protein digestion was reached, compared to 6% for a wheat-based pasta enriched with 35% fava  
457 bean flour. While proteolysis is expressed in different terms throughout literature, and values are  
458 thus hard to compare, these results indicate that lentil proteins in a 100% (raw-milled) lentil-based  
459 pasta might be slightly more accessible to hydrolytic enzymes as compared to covalently linked  
460 gluten in wheat-based pasta.

461 During the small intestinal phase, the formation of bioaccessible protein ( $\text{NH}_2\text{TCA}$  and  $\text{NH}_2\text{TCA}_{\text{hydro}}$ )  
462 followed a fractional conversion behavior, with the rate of proteolysis decreasing with proceeding  
463 digestion. While no plateau was reached within 180 min of simulation, the data were anyhow  
464 modelled using the fractional conversion model to allow comparison of the proteolytic behavior  
465 of the different considered samples, with estimated parameters shown in **Table 3**. While the  
466 modelled curves fit the data well, the estimated final values require cautious interpretation.

467 At each considered digestion time during the gastric and small intestinal phases, the extent of  
468 protein hydrolysis was higher for 100%RM compared to the 30%ICC and 30%WL pasta. In  
469 literature, bioencapsulation of protein in intact pulse cotyledon cells has indeed been linked to  
470 decreased protein digestibility (Pälchen, Van Den Wouwer, et al., 2022; Zahir et al., 2018).  
471 30%ICC and 30%WL pasta showed a quite similar behavior in terms of bioaccessible protein  
472 ( $\text{NH}_2\text{TCA}$ ) release, while a higher plateau was observed for 30%WL compared to 30%ICC pasta in  
473 terms of hydrolyzed bioaccessible protein ( $\text{NH}_2\text{TCA}_{\text{hydro}}$ ). This difference could be attributed to the  
474 lower fraction of individual cells with entrapped macronutrients, and the relatively higher fraction  
475 of seed coat material possibly disrupting the protein matrix, in the WL powder (Dodi et al., 2021;  
476 Laleg, Barron, et al., 2016). However, upon long digestion times, the observed difference in  
477 digestion extent ( $C_f$ ) between 100%RM, 30%ICC, and 30%WL became statistically insignificant  
478 in terms of amino acid constituents ( $\text{NH}_2\text{TCA}_{\text{hydro}}$ ). While the partial substitution of raw-milled  
479 flour by ICC or WL powder in lentil pasta thus significantly decreased starch digestion kinetics  
480 (*section 3.4*), the difference in formation of bioaccessible protein is rather limited, especially in  
481 the case of 30%WL pasta.

482 Generally, the evolution of hydrolyzed bioaccessible protein ( $\text{NH}_2\text{TCA}_{\text{hydro}}$ ) in the 100%RM pasta  
483 followed a similar trend compared to a heat-treated suspension of raw-milled lentil flour (Duijsens,

484 Pälchen, De Coster, et al., 2022), reaching similar final values but with a significantly lower rate  
485 constant. It can therefore be expected that the pasta structure would have a (limited but) rate-  
486 determining effect on the conversion of protein into absorbable units in absolute terms.

487 Protein digestibility of 100%RM was higher than for a reference wheat-based pasta (approximately  
488 20% upon 120 min small intestinal digestion, *data in Supplementary material 3*). An increased  
489 protein digestibility of 100% pulse-based pasta compared to a commercial wheat-based pasta could  
490 be expected due to the formation of a weaker (non covalently bound soluble) protein network and  
491 its disruption by seed coat particles and fiber. In literature, protein digestibility values of about  
492 42% were found for wheat semolina pasta, and 46% for wheat pasta substituted with 35% fava  
493 bean flour (Laleg, Barron, et al., 2016). However, comparison with the current data is difficult due  
494 to different applied methods for digestion simulation and analysis. Moreover, absolute levels of  
495 protein digestibility may be affected by differences in pasta diameter and compactness of the pasta,  
496 in turn affected by the manufacturing steps as well (*e.g.*, manually made *versus* extrusion, drying  
497 temperature) (Petitot et al., 2009). More insight into the protein network formed in these pasta  
498 samples as well as its exact hydrolysis patterns could be obtained through *e.g.*, HPLC-SEC  
499 (Duijsens et al., 2023; Petitot et al., 2009).

### 500 **3.6 Mineral bioaccessibility of pasta**

501 The Ca, Mg, Fe, and Zn bioaccessibilities of cooked 100%RM, 30%ICC, and 30%WL pasta are  
502 shown in **Figure 2B**. In accordance with data reported on different pulse types (Gwala et al., 2020;  
503 Rousseau, Celus, et al., 2020), mineral bioaccessibility did not reach 100% in the pasta samples  
504 and significant mineral chelation thus occurred.

505 **Ca** bioaccessibility reached values between 60 and 72% and did not significantly differ between  
506 different pasta samples. Correspondingly, a Ca bioaccessibility of 59% was found for green lentils



507 (Suliburska & Krejpcio, 2014), and similar values were reported for cooked Bambara groundnuts  
508 and common beans (Gwala et al., 2020; Rousseau, Celus, et al., 2020), indicating no significant  
509 effect of lentil flour incorporation into pasta on Ca bioaccessibility (in %).

510 **Mg** was found the most bioaccessible mineral in lentil-based pasta in this study (65 to 90%), in  
511 similarity to several other cooked pulses and attributed to its inherent lower potential to interact  
512 with antinutrients such as pectin (Gwala et al., 2020; Rousseau, Celus, et al., 2020; Suliburska &  
513 Krejpcio, 2014) (see *section 3.3*).

514 **Fe** bioaccessibility was low in all samples (10 to 14%). Varying values have been reported for Fe  
515 bioaccessibility in literature (Gwala et al., 2020; Hemalatha, Platel, & Srinivasan, 2007; Rousseau,  
516 Celus, et al., 2020; Suliburska & Krejpcio, 2014). Fe bioaccessibility was shown to be significantly  
517 reduced by complexation by phytic acid in pulses and cereals (Hemalatha et al., 2007; Moore et  
518 al., 2018).

519 The determined **Zn** bioaccessibility is in line with values determined for other pulses (Gwala et  
520 al., 2020; Rousseau, Celus, et al., 2020). Importantly, it should be taken into account that  
521 competition effects could arise, as Zn chelation by pectin was found to decrease upon increasing  
522 Ca concentration (Rousseau et al., 2019). In the lentil-based pastas of this study, the Ca content is  
523 over 20 times higher as compared to Zn, and competition for chelation is thus a plausible  
524 mechanism.

525 The decrease in Mg and Zn bioaccessibility upon incorporation of ingredients with cellular  
526 intactness (100%RM>30%WL>30%ICC) is remarkable. In this context, Rousseau, Pallares  
527 Pallares et al. (2020) identified that, rather than cellular intactness, the presence of mineral  
528 antinutrients in foods (*i.e.*, phytic acid and pectin) caused mineral chelation reducing

529 bioaccessibility in cooked common beans. Therefore, a possible explanation could be that thermal  
530 pretreatment of ingredients (ICC and WL) influenced the composition and ratio of antinutrients  
531 and minerals, ultimately affecting bioaccessibility. During thermal pretreatment of ICC and WL,  
532 more bioaccessible (soluble and unbound) minerals could have preferably leached out compared  
533 to chelated minerals. Moreover, mineral bioaccessibility has been described to be affected by the  
534 formation of Zn-protein complexes (Hemalatha et al., 2007). Consequentially, a higher extent of  
535 (gastric) protein solubilization in an open system (i.e. 100%RM) could explain a higher  
536 bioaccessibility as compared to systems with cellular intactness (30%ICC and 30%WL), as  
537 postulated by Gwala, Kyomugasho, et al. (2020). However, while the effect of gastric proteolysis  
538 was not studied, no effect of (small intestinal) digestion time was observed on mineral  
539 bioaccessibility (*data not shown*).

540 To determine if significant amounts of minerals could be accessible for absorption in the small  
541 intestine upon the consumption of one portion (100g) of cooked pasta (mineral content shown in  
542 **Figure 2A**), bioaccessibility was expressed in absolute amounts and in terms of the average daily  
543 requirements (ADR) (*data in Supplementary material 4*). One portion could offer around 5, 10-  
544 13, 12-15, and 5-9 % of the ADR of Ca, Mg, Zn, and Fe, respectively. Especially for Fe, 100 g  
545 pasta would deliver an appreciable bioaccessible amount (up to 15% of ADR). These values are  
546 in accordance with previously reported values for cooked whole common beans (Duijsens et al.,  
547 2021; Rousseau, Celus, et al., 2020).

548 Generally, it can be concluded that while lentils contain significant amounts of minerals (**Figure**  
549 **2A**), the mineral quality of the produced pastas is limited. Based on literature, a possible strategy  
550 for increasing mineral bioaccessibility in lentil-based pasta could be to produce ingredients from

551 dehulled lentils, decreasing the total antinutrient, but also mineral and fiber content (Rousseau,  
552 Celus, et al., 2020).

#### 553 **4 Conclusion**

554 The effect of incorporating ingredients with cellular intactness into raw-milled lentil pasta flour  
555 formulations (100%RM, 30%ICC, and 30%WL) was investigated on cooking properties,  
556 composition, macronutrient digestibility, and mineral bioaccessibility.

557 While the effects on cooking properties were limited, 30%ICC and 30%WL had slightly higher  
558 protein and starch, but lower fiber and ash contents, compared 100%RM pasta. 30%ICC and  
559 30%WL pasta showed a slowed amylolysis compared to 100%RM pasta. The pasta structure could  
560 be identified as the major rate-determining physical barrier for amylolysis, enhanced by partial  
561 nutrient bioencapsulation. The attenuation of proteolysis was attributed to bioencapsulation as  
562 well, while the effect on final protein digestibility was limited. The incorporation of a (partially)  
563 cellular ingredient into the pasta formulation moderately decreased Zn and Mg bioaccessibility,  
564 while this was not the case for Ca and Fe. To conclude, the lentil-based pastas prepared here have  
565 a large potential as a food with improved nutritional properties (high in digestible protein and  
566 slow(er) starch digestion). However, similarly to cooked pulses, their potential as sources of  
567 bioaccessible minerals is limited.

568 Further investigation should lead to pastas with improved techno-functional properties (*e.g.*,  
569 textural properties) and insights into (sensorial) consumer acceptability of these products. The use  
570 of different flour blends (*e.g.*, wheat semolina combined with ICC or WL powder) could deliver  
571 pastas with improved cooking quality and interesting nutritional properties. In the context of an  
572 industrial application, it should be confirmed if nutrient bioencapsulation prevails upon more harsh

573 processing as well, *e.g.*, extrusion and high temperature drying. Besides, *in vivo* studies should be  
574 carried out, testing the current findings in terms of physiologically relevant parameters such as  
575 glycemic index and satiety/satiation.

## 576 **Acknowledgements**

577 D. Duijsens is a PhD researcher funded by the Research Foundation Flanders (FWO - Grant no.  
578 1S23321N). S.H.E. Verkempinck is a Postdoctoral Researcher funded by the Research Foundation  
579 Flanders (FWO - Grant no. 1222420N). K. Pälchen is a PhD fellow funded by European Union's  
580 Horizon 2020 Research and Innovation Program under the Marie Skłodowska-Curie (Grant no.  
581 765415). The authors acknowledge the financial support of the KU Leuven Research Fund.

## 582 **Conflict of interest**

583 None

584

585 **References**

- 586 Bajka, B. H., Pinto, A. M., Ahn-Jarvis, J., Ryden, P., Perez-Moral, N., van der Schoot, A., Stocchi,  
587 C., Bland, C., Berry, S. E., Ellis, P. R., & Edwards, C. H. (2021). The impact of replacing  
588 wheat flour with cellular legume powder on starch bioaccessibility, glycaemic response and  
589 bread roll quality: A double-blind randomised controlled trial in healthy participants. *Food*  
590 *Hydrocolloids*, 114(December 2020), 106565.  
591 <https://doi.org/10.1016/j.foodhyd.2020.106565>
- 592 Brodkorb, A., Egger, L., Alminger, M., Alvito, P., Assunção, R., Ballance, S., Bohn, T., Bourlieu-  
593 Lacanal, C., Boutrou, R., Carrière, F., Clemente, A., Corredig, M., Dupont, D., Dufour, C.,  
594 Edwards, C., Golding, M., Karakaya, S., Kirkhus, B., Le Feunteun, S., ... Recio, I. (2019).  
595 INFOGEST static in vitro simulation of gastrointestinal food digestion. *Nature Protocols*,  
596 14(4), 991–1014. <https://doi.org/10.1038/s41596-018-0119-1>
- 597 De Almeida Costa, G. E., Da Silva Queiroz-Monici, K., Pissini Machado Reis, S. M., & De  
598 Oliveira, A. C. (2006). Chemical composition, dietary fibre and resistant starch contents of  
599 raw and cooked pea, common bean, chickpea and lentil legumes. *Food Chemistry*, 94(3),  
600 327–330. <https://doi.org/10.1016/j.foodchem.2004.11.020>
- 601 Dhital, S., Gidley, M. J., & Warren, F. J. (2015). Inhibition of  $\alpha$ -amylase activity by cellulose:  
602 Kinetic analysis and nutritional implications. *Carbohydrate Polymers*, 123, 305–312.  
603 <https://doi.org/10.1016/j.carbpol.2015.01.039>
- 604 Dodi, R., Bresciani, L., Biasini, B., Cossu, M., Scazzina, F., Taddei, F., D'egidio, M. G., Dall'asta,  
605 M., & Martini, D. (2021). Traditional and non-conventional pasta-making processes: Effect  
606 on in vitro starch digestibility. *Foods*, 10(5), 1–10. <https://doi.org/10.3390/foods10050921>

607 Duijsens, D., Pälchen, K., De Coster, A., Verkempinck, S. H. E., Hendrickx, M. E., & Grauwet,  
608 T. (2022). Effect of manufacturing conditions on in vitro starch and protein digestibility of  
609 (cellular) lentil-based ingredients. *Food Research International*, 158(August 2022).  
610 <https://doi.org/10.1016/j.foodres.2022.111546>

611 Duijsens, D., Pälchen, K., Guevara-Zambrano, J. ., Verkempinck, S. H. ., Infantes-Garcia, M. .,  
612 Hendrickx, M. ., Van Loey, A., & Grauwet, T. (2022). Strategic choices for in vitro food  
613 digestion methodologies enabling food digestion design. *Trends in Food Science &*  
614 *Technology*, 126, 61–72. <https://doi.org/10.1016/j.tifs.2022.06.017>

615 Duijsens, D., Gwala, S., Pallares, A. P., Pälchen, K., Hendrickx, M., & Grauwet, T. (2021). How  
616 postharvest variables in the pulse value chain affect nutrient digestibility and bioaccessibility.  
617 *Comprehensive Reviews in Food Science and Food Safety*, June, 1–30.  
618 <https://doi.org/10.1111/1541-4337.12826>

619 Duijsens, D., Pälchen, K., Verkempinck, S., Guevara Zambrano, J., Hendrickx, M., Van Loey, A.,  
620 & Grauwet, T. (2023). Size exclusion chromatography to evaluate in vitro proteolysis: a case  
621 study on the impact of microstructure in pulse powders. *Food Chemistry*, 418, 135709.  
622 <https://doi.org/10.1016/j.foodchem.2023.135709>

623 Edwards, C. H., Cochetel, N., Setterfield, L., Perez-Moral, N., & Warren, F. J. (2019). A single-  
624 enzyme system for starch digestibility screening and its relevance to understanding and  
625 predicting the glycaemic index of food products. *Food and Function*, 10(8), 4751–4760.  
626 <https://doi.org/10.1039/c9fo00603f>

627 Freitas, D., & Le Feunteun, S. (2019). Oro-gastro-intestinal digestion of starch in white bread,  
628 wheat-based and gluten-free pasta: Unveiling the contribution of human salivary  $\alpha$ -amylase.

629 *Food Chemistry*, 274(August 2018), 566–573.  
630 <https://doi.org/10.1016/j.foodchem.2018.09.025>

631 Galani, Y. J. H., Orfila, C., & Gong, Y. Y. (2022). A review of micronutrient deficiencies and  
632 analysis of maize contribution to nutrient requirements of women and children in Eastern and  
633 Southern Africa. *Critical Reviews in Food Science and Nutrition*, 62(6), 1568–1591.  
634 <https://doi.org/10.1080/10408398.2020.1844636>

635 Gallegos-Infante, J. A., Rocha-Guzman, N. E., Gonzalez-Laredo, R. F., Ochoa-Martínez, L. A.,  
636 Corzo, N., Bello-Perez, L. A., Medina-Torres, L., & Peralta-Alvarez, L. E. (2010). Quality of  
637 spaghetti pasta containing Mexican common bean flour (*Phaseolus vulgaris* L.). *Food*  
638 *Chemistry*, 119(4), 1544–1549. <https://doi.org/10.1016/j.foodchem.2009.09.040>

639 Garcia-Valle, D. E., Bello-Pérez, L. A., Agama-Acevedo, E., & Alvarez-Ramirez, J. (2021).  
640 Structural characteristics and in vitro starch digestibility of pasta made with durum wheat  
641 semolina and chickpea flour. *Lwt*, 145(January). <https://doi.org/10.1016/j.lwt.2021.111347>

642 Giuberti, G., Gallo, A., Cerioli, C., Fortunati, P., & Masoero, F. (2015). Cooking quality and starch  
643 digestibility of gluten free pasta using new bean flour. *Food Chemistry*, 175, 43–49.  
644 <https://doi.org/10.1016/j.foodchem.2014.11.127>

645 Gwala, S., Kyomugasho, C., Wainaina, I., Rousseau, S., Hendrickx, M., & Grauwet, T. (2020).  
646 Ageing, dehulling and cooking of Bambara groundnuts: Consequences for mineral retention  
647 and: In vitro bioaccessibility. *Food and Function*, 11(3), 2509–2521.  
648 <https://doi.org/10.1039/c9fo01731c>

649 Gwala, S., Wainana, I., Pallares Pallares, A., Kyomugasho, C., Hendrickx, M., & Grauwet, T.  
650 (2019). Texture and interlinked post-process microstructures determine the in vitro starch

651 digestibility of Bambara groundnuts with distinct hard-to-cook levels. *Food Research*  
652 *International*, 120(February), 1–11. <https://doi.org/10.1016/j.foodres.2019.02.022>

653 Hemalatha, S., Platel, K., & Srinivasan, K. (2007). Influence of heat processing on the  
654 bioaccessibility of zinc and iron from cereals and pulses consumed in India. *Journal of Trace*  
655 *Elements in Medicine and Biology*, 21(1), 1–7. <https://doi.org/10.1016/j.jtemb.2006.10.002>

656 Henn, K., Goddyn, H., Bøye Olsen, S., Bredie, W. L. P., Olsen, S. B., & Bredie, W. L. P. (2021).  
657 Identifying behavioral and attitudinal barriers and drivers to promote consumption of pulses:  
658 A quantitative survey across five European countries. *Food Quality and Preference*, 98,  
659 104455. <https://doi.org/10.1016/j.foodqual.2021.104455>

660 Hoebler, C., Karinhi, A., Devaux, M.-F. F., Guillon, F., Gallant, D. J. G. G., Bouchet, B.,  
661 Melegari, C., & Barry, J.-L. L. (1998). Physical and chemical transformations of cereal food  
662 during oral digestion in human subjects. *British Journal of Nutrition*, 80(5), 429–436.  
663 <https://doi.org/10.1017/s0007114598001494>

664 Janssen, F., Wouters, A. G. B., Pareyt, B., Gerits, L. R., Delcour, J. A., Waelkens, E., & Derua, R.  
665 (2018). Wheat (*Triticum aestivum* L.) lipid species distribution in the different stages of  
666 straight dough bread making. *Food Research International*, 112(May), 299–311.  
667 <https://doi.org/10.1016/j.foodres.2018.06.038>

668 Laleg, K., Barron, C., Santé-Lhoutellier, V., Walrand, S., & Micard, V. (2016). Protein enriched  
669 pasta: Structure and digestibility of its protein network. *Food and Function*, 7(2), 1196–1207.  
670 <https://doi.org/10.1039/c5fo01231g>

671 Laleg, K., Cassan, D., Barron, C., Prabhasankar, P., & Micard, V. (2016). Structural, culinary,  
672 nutritional and anti-nutritional properties of high protein, gluten free, 100% legume pasta.



673 *PLoS ONE*, 11(9), 1–19. <https://doi.org/10.1371/journal.pone.0160721>

674 Lombardi-Boccia, G., Lucarini, M., Di Lullo, G., Del Puppo, E., Ferrari, A., & Carnovale, E.  
675 (1998). Dialysable, soluble and fermentable calcium from beans (*Phaseolus vulgaris* L.) as  
676 model for in vitro assessment of the potential calcium availability. *Food Chemistry*, 61(1–2),  
677 167–171. [https://doi.org/10.1016/S0308-8146\(97\)00040-X](https://doi.org/10.1016/S0308-8146(97)00040-X)

678 Moore, K. L., Rodríguez-Ramiro, I., Jones, E. R., Jones, E. J., Rodríguez-Celma, J., Halsey, K.,  
679 Domoney, C., Shewry, P. R., Fairweather-Tait, S., & Balk, J. (2018). The stage of seed  
680 development influences iron bioavailability in pea (*Pisum sativum* L.). *Scientific Reports*,  
681 8(1), 1–11. <https://doi.org/10.1038/s41598-018-25130-3>

682 Noordraven, L. E. C., Bernaerts, T., Mommens, L., Hendrickx, M. E., & Van Loey, A. M. (2021).  
683 Impact of cell intactness and starch state on the thickening potential of chickpea flours in  
684 water-flour systems. *LWT*, 146(March), 111409. <https://doi.org/10.1016/j.lwt.2021.111409>

685 Pälchen, K., Bredie, W. L. P., Duijsens, D., Alfie, A. I., Hendrickx, M., Loey, A. Van, Raben, A.,  
686 & Grauwet, T. (2022). Effect of processing and microstructural properties of chickpea-flours  
687 on in vitro digestion and appetite sensations. *Food Research International*, 111245.  
688 <https://doi.org/10.1016/j.foodres.2022.111245>

689 Pälchen, K., Van Den Wouwer, B., Duijsens, D., Hendrickx, M. E., Van Loey, A., & Grauwet, T.  
690 (2022). Utilizing Hydrothermal Processing to Align Structure and In Vitro Digestion Kinetics  
691 between Three Different Pulse Types. *Foods*, 11(2), 206.  
692 <https://doi.org/10.3390/foods11020206>

693 Patel, M. J., & Chakrabarti-Bell, S. (2013). Flour quality and dough elasticity: Dough sheetability.  
694 *Journal of Food Engineering*, 115(3), 371–383.

695 <https://doi.org/10.1016/j.jfoodeng.2012.10.038>

696 Petitot, M., Barron, C., Morel, M. H., & Micard, V. (2010). Impact of Legume Flour Addition on  
697 Pasta Structure: Consequences on Its In Vitro Starch Digestibility. *Food Biophysics*, 5(4),  
698 284–299. <https://doi.org/10.1007/s11483-010-9170-3>

699 Petitot, M., Brossard, C., Barron, C., Larré, C., Morel, M. H., & Micard, V. (2009). Modification  
700 of pasta structure induced by high drying temperatures. Effects on the in vitro digestibility of  
701 protein and starch fractions and the potential allergenicity of protein hydrolysates. *Food*  
702 *Chemistry*, 116(2), 401–412. <https://doi.org/10.1016/j.foodchem.2009.01.001>

703 Petitot, M., & Micard, V. (2010). Legume-Fortified Pasta. Impact of Drying and Precooking  
704 Treatments on Pasta Structure and Inherent In Vitro Starch Digestibility. *Food Biophysics*,  
705 5(4), 309–320. <https://doi.org/10.1007/s11483-010-9180-1>

706 Platel, K., & Srinivasan, K. (2016). Bioavailability of Micronutrients from Plant Foods : An  
707 Update Bioavailability of Micronutrients from Plant Foods : An Update. *Critical Reviews in*  
708 *Food Science and Nutrition* ISSN:, 56(10), 1608–1619.  
709 <https://doi.org/10.1080/10408398.2013.781011>

710 Rosa-Sibakov, N., Heiniö, R. L., Cassan, D., Holopainen-Mantila, U., Micard, V., Lantto, R., &  
711 Sozer, N. (2016). Effect of bioprocessing and fractionation on the structural, textural and  
712 sensory properties of gluten-free faba bean pasta. *LWT - Food Science and Technology*, 67,  
713 27–36. <https://doi.org/10.1016/j.lwt.2015.11.032>

714 Rousseau, S., Celus, M., Duijsens, D., Gwala, S., Hendrickx, M., & Grauwet, T. (2020). The  
715 impact of postharvest storage and cooking time on mineral bioaccessibility in common beans.  
716 *Food and Function*, 11(9), 7584–7595. <https://doi.org/10.1039/d0fo01302a>

717 Rousseau, S., Kyomugasho, C., Celus, M., Yeasmen, N., Hendrickx, M. E., & Grauwet, T. (2019).  
718 Zinc bioaccessibility is affected by the presence of calcium ions and degree of  
719 methylesterification in pectin-based model systems. *Food Hydrocolloids*, 90(December  
720 2018), 206–215. <https://doi.org/10.1016/j.foodhyd.2018.12.019>

721 Rousseau, S., Pallares Pallares, A., Vancoillie, F., Hendrickx, M., & Grauwet, T. (2020). Pectin  
722 and phytic acid reduce mineral bioaccessibility in cooked common bean cotyledons  
723 regardless of cell wall integrity. *Food Research International*, 137(May), 109685.  
724 <https://doi.org/10.1016/j.foodres.2020.109685>

725 Suliburska, J., & Krejpcio, Z. (2014). Evaluation of the content and bioaccessibility of iron, zinc,  
726 calcium and magnesium from groats, rice, leguminous grains and nuts. *Journal of Food  
727 Science and Technology*, 51(3), 589–594. <https://doi.org/10.1007/s13197-011-0535-5>

728 Warren, F. J., Zhang, B., Waltzer, G., Gidley, M. J., & Dhital, S. (2015). The interplay of  $\alpha$ -  
729 amylase and amyloglucosidase activities on the digestion of starch in in vitro enzymic  
730 systems. *Carbohydrate Polymers*, 117, 185–191.  
731 <https://doi.org/10.1016/j.carbpol.2014.09.043>

732 Zahir, M. A., Fogliano, V., & Capuano, E. (2018). Food matrix and processing modulates in vitro  
733 protein digestibility in soybean. *Food & Function*, 9(12), 6326–6336.  
734 <https://doi.org/10.1039/C8FO01385C>

735

Table 1: Cooking properties of 100% RM, 30%ICC, and 30%WL lentil pasta produced in this study. Dough moisture addition, optimal cooking time (OCT), dry matter loss, protein loss, and starch loss are indicated in % dry matter  $\pm$  standard deviation.

Lentil pasta	Dough moisture addition (%)	OCT (min)	Water uptake (%)	Dry matter loss (%)	Protein loss (%)	Starch loss (%)
100%RM	49	15	291.4 $\pm$ 0.2	15.3 $\pm$ 0.1	9.1 $\pm$ 0.1	17.0 $\pm$ 0.1
30%ICC	74	12	297.2 $\pm$ 0.9	10.2 $\pm$ 0.2	2.3 $\pm$ 0.2	6.0 $\pm$ 0.2
30% WL	70	12	289.5 $\pm$ 1.7	16.0 $\pm$ 0.4	8.7 $\pm$ 0.4	13.6 $\pm$ 0.4

100%RM: lentil pasta made of 100% raw-milled lentil flour; 30%ICC: lentil pasta made of 70% raw-milled flour and 30% isolated cotyledon cell powder; 30%WL: lentil pasta made of 70% raw-milled and 30% whole precooked lentil powder.

CONFIDENTIAL

Table 2: Chemical composition (g/100g dry matter (DM)) of uncooked and cooked lentil pasta samples. Different superscript letters within a column indicate significant differences between the mean values (Tukey's range test  $p < 0.05$  except for 95% confidence interval for calculated fiber-rich residue).

	Lentil pasta	Dry matter (g/100g)	Starch (g/100g DM)	Protein (g/100g DM)	Ash (g/100g DM)	Lipid (g/100g DM)	Fiber-rich residue <sup>1</sup> (g/100g DM)
Uncooked	100%RM	92.37 ± 0.01 <sup>a</sup>	44.56 ± 0.05 <sup>d</sup>	20.64 ± 0.18 <sup>c</sup>	2.80 ± 0.01 <sup>a</sup>	2.82 ± 0.10 <sup>b,c</sup>	29.17 ± 0.34 <sup>a</sup>
	30%ICC	91.03 ± 0.01 <sup>b</sup>	50.20 ± 0.61 <sup>c</sup>	20.93 ± 0.43 <sup>c,b</sup>	1.99 ± 0.01 <sup>b</sup>	2.57 ± 0.23 <sup>c</sup>	24.31 ± 0.79 <sup>b</sup>
	30%WL	91.11 ± 0.01 <sup>c</sup>	46.24 ± 0.58 <sup>d,b</sup>	21.25 ± 0.06 <sup>b</sup>	2.06 ± 0.01 <sup>b</sup>	2.67 ± 0.20 <sup>c</sup>	27.78 ± 0.63 <sup>a</sup>
Cooked	100%RM	19.98 ± 0.01 <sup>d</sup>	45.37 ± 0.33 <sup>d</sup>	22.18 ± 0.01 <sup>a</sup>	0.88 ± 0.01 <sup>c</sup>	3.59 ± 0.39 <sup>a,b</sup>	27.99 ± 0.59 <sup>a</sup>
	30%ICC	20.58 ± 0.00 <sup>d</sup>	52.56 ± 0.16 <sup>a</sup>	22.76 ± 0.05 <sup>a</sup>	0.74 ± 0.01 <sup>c</sup>	3.49 ± 0.44 <sup>a,b</sup>	20.447 ± 0.49 <sup>c</sup>
	30%WL	19.66 ± 0.00 <sup>d</sup>	47.56 ± 0.26 <sup>b</sup>	23.08 ± 0.02 <sup>a</sup>	0.58 ± 0.01 <sup>c</sup>	3.91 ± 0.24 <sup>a</sup>	24.87 ± 0.35 <sup>b</sup>

<sup>1</sup>Calculated by difference, containing both fibers and sugars (including raffinose family oligosaccharides)

100%RM: lentil pasta made of 100% raw-milled lentil flour; 30%ICC: lentil pasta made of 70% raw-milled flour and 30% isolated cotyledon cell powder; 30%WL: lentil pasta made of 70% raw-milled and 30% whole precooked lentil powder.

Table 3: Estimated kinetic parameters of the fractional conversion model for in vitro amylolysis and proteolysis of 100%RM, 30%ICC, and 30%WL pasta cooked to their optimal cooking time. Proteolysis is expressed in terms of readily bioaccessible protein ( $\text{NH}_2\text{TCA}$ , %) and hydrolyzed readily bioaccessible protein ( $\text{NH}_2\text{TCA}_{\text{hydro}}$ , %). Estimated kinetic parameters include rate constant ( $k$ ,  $\text{min}^{-1}$ ) and final degree of amylolysis/proteolysis ( $C_f$ , %). Values are estimates  $\pm$  standard error. For one type of analysis, different superscript letters within a column indicate significant differences between the mean values (95% confidence intervals).

Amylolysis						
Lentil pasta	$k$ ( $\text{min}^{-1}$ )	$C_f$ (%)	$R^2_{\text{adj}}$	$V_{\text{initial}}$ ( $\% \text{min}^{-1}$ )	$C_{90}$ (%)	$C_{120}$ (%)
100%RM	$0.035 \pm 0.005^a$	$102.3 \pm 5.3^a$	0.99	$3.55 \pm 0.55^a$	$97.8 \pm 3.8^a$	$100.7 \pm 4.5^a$
30%ICC	$0.023 \pm 0.003^a$	$77.286 \pm 3.5^b$	0.99	$1.75 \pm 0.22^c$	$67.3 \pm 1.8^c$	$72.2 \pm 2.2^c$
30% WL	$0.027 \pm 0.003^a$	$85.99 \pm 3.3^{a,b}$	0.99	$2.33 \pm 0.27^b$	$78.5 \pm 2.1^b$	$82.7 \pm 2.5^b$
Proteolysis						
Lentil pasta	Readily bioaccessible protein ( $\text{NH}_2\text{TCA}$ )			Hydrolyzed readily bioaccessible protein ( $\text{NH}_2\text{TCA}_{\text{hydro}}$ )		
	$k$ ( $\text{min}^{-1}$ )	$C_f$ (%)	$R^2_{\text{adj}}$	$k$ ( $\text{min}^{-1}$ )	$C_f$ (%)	$R^2_{\text{adj}}$
100%RM	$0.013 \pm 0.001^a$	$42.7 \pm 1.5^a$	0.99	$0.014 \pm 0.003^{a,b}$	$99.6 \pm 5.6^a$	0.99
30%ICC	$0.020 \pm 0.003^a$	$26.8 \pm 1.1^b$	0.99	$0.010 \pm 0.001^b$	$91.1 \pm 5.4^a$	0.99
30% WL	$0.006 \pm 0.001^b$	$44.7 \pm 3.8^a$	0.99	$0.023 \pm 0.002^a$	$91.2 \pm 2.5^a$	0.99

100%RM: lentil pasta made of 100% raw-milled lentil flour; 30%ICC: lentil pasta made of 70% raw-milled flour and 30% isolated cotyledon cell powder; 30%WL: lentil pasta made of 70% raw-milled and 30% whole precooked lentil powder.

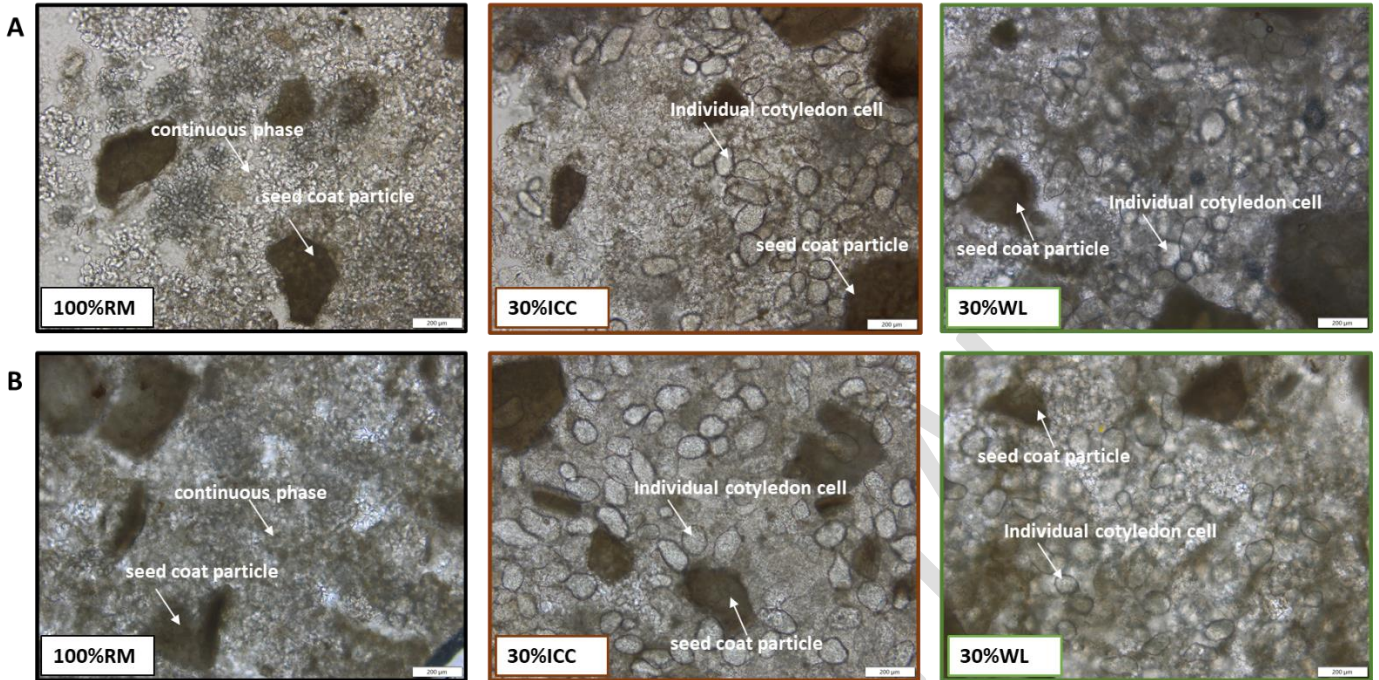


Figure 1: Representative micrographs of 100%RM (-), 30%ICC (-), 30%WL (-) pasta cooked to the optimal cooking time, A) before, and B) upon 90 minutes of in vitro small intestinal digestion (magnification 10x, scale bar 200 µm). Arrows indicate the continuous phase, seed coat particles, and individual cotyledon cells.

CONFIDENTIAL

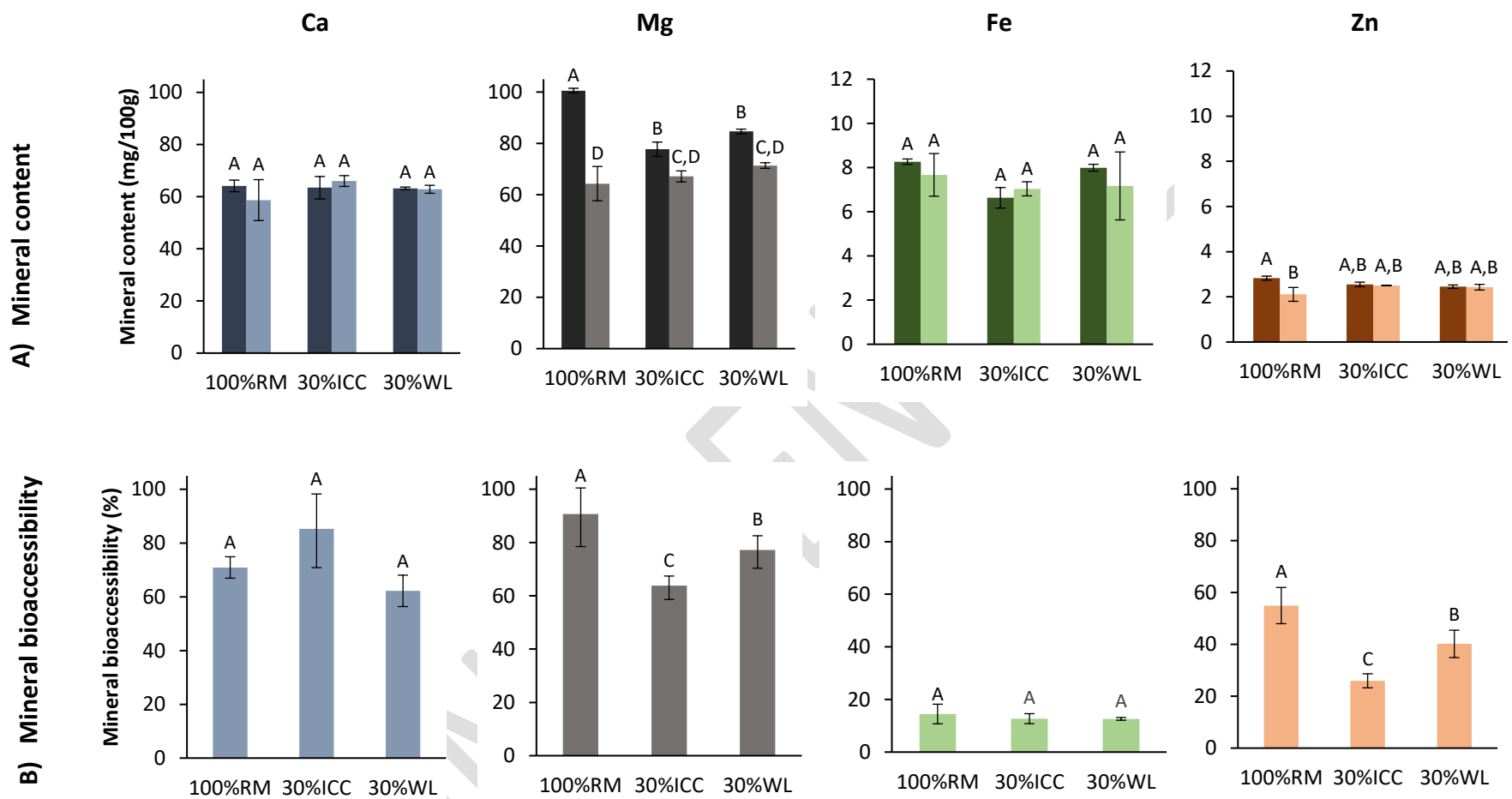


Figure 2: A) Ca (■/■), Mg (■/■) and B) Fe (■/■), and Zn (■/■) content (in mg/100g dry matter) of 100%RM, 30%ICC, and 30%WL lentil pasta before and upon cooking, respectively. B) Ca (■), Mg (■), Fe (■), and Zn (■) bioaccessibility in 100%RM, 30%ICC, and 30%WL lentil pasta cooked to their optimal cooking time. Dark colors indicate mineral content before cooking, while the bright colors indicate the mineral content/bioaccessibility of the corresponding pasta after cooking for the determined optimal cooking time. For mineral content (A) and bioaccessibility (B), within a mineral type, different letters indicate significant difference of the mean content (Tukey's range test,  $p < 0.05$ ).



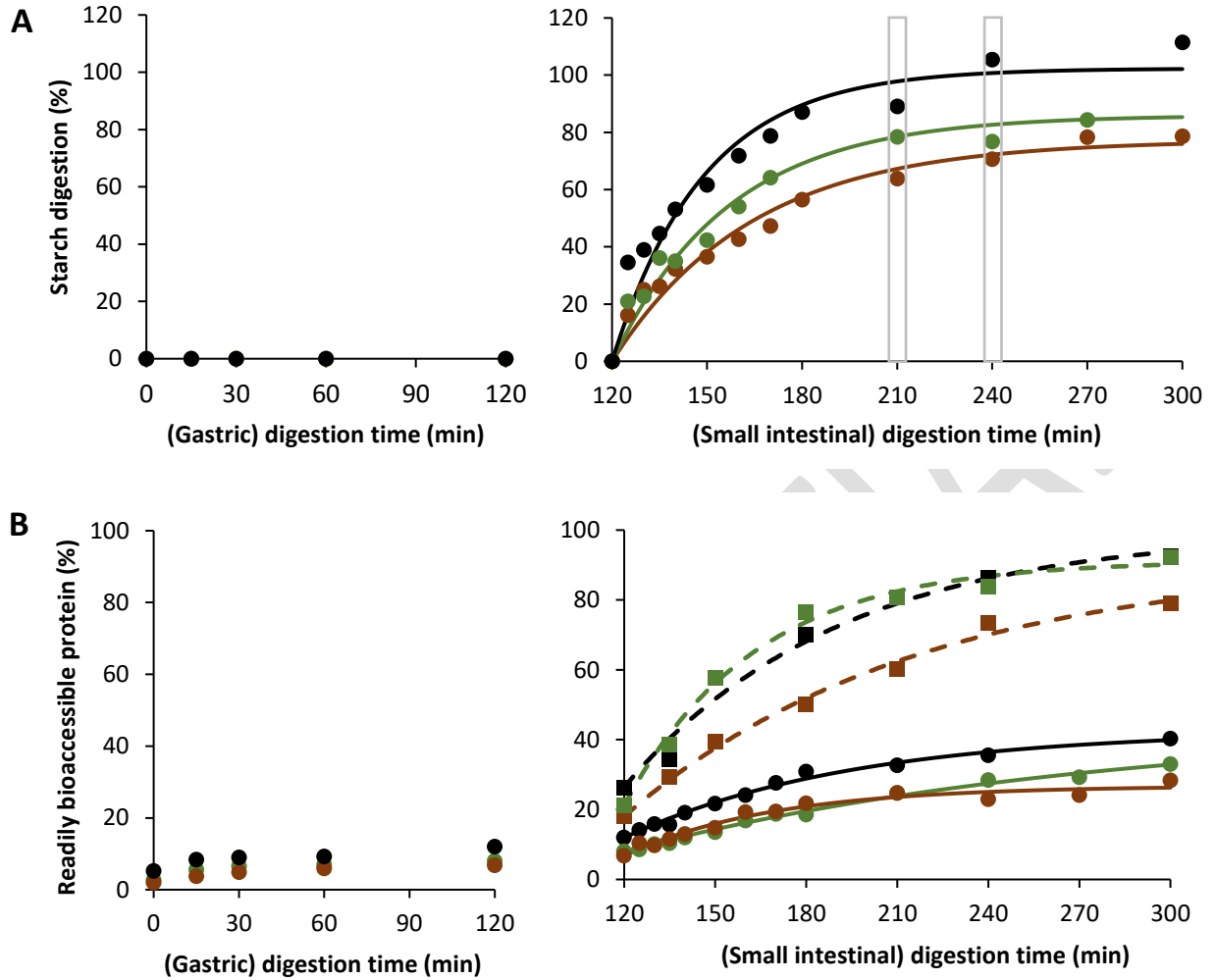


Figure 3: A) *In vitro* amylolysis of 100%RM (●), 30%ICC (●), and 30%WL (●) pasta cooked to its optimal cooking time. B) *In vitro* proteolysis of 100%RM (●), 30%ICC (●), and 30%WL (●) pasta cooked to its optimal cooking time in terms of bioaccessible protein ( $NH_{2TCA}$ , %, ●) and hydrolyzed bioaccessible protein ( $NH_{2TCA,hydr}$ , %, ■). Points are experimentally determined data. Lines represent the data modelled using the fractional conversion model. Grey boxes indicate amylolysis levels upon 90 and 120 min of small intestinal digestion.

## Supplementary material 1

Table S1: Indicated and values measured via ICP-OES (mean  $\pm$  stdev) of certified reference materials BCR-129 and BCR-679.

	Indicated values (mg/g)		Measured values (mg/g)	
	Hay powder BCR-129	Cabbage powder BCR-679	Hay powder BCR-129	Cabbage powder BCR-679
Fe	0.055	0.114	0.0433 $\pm$ 0.0063	0.0847 $\pm$ 0.0032
Mg	1.362	1.45	1.192 $\pm$ 0.053	1.269 $\pm$ 0.023
Zn	0.0797	0.0321	0.0723 $\pm$ 0.0031	0.0245 $\pm$ 0.0019
Ca	7.768	6.4	6.537 $\pm$ 1.170	5.467 $\pm$ 0.2721

CONFIDENTIAL

## Supplementary material 2

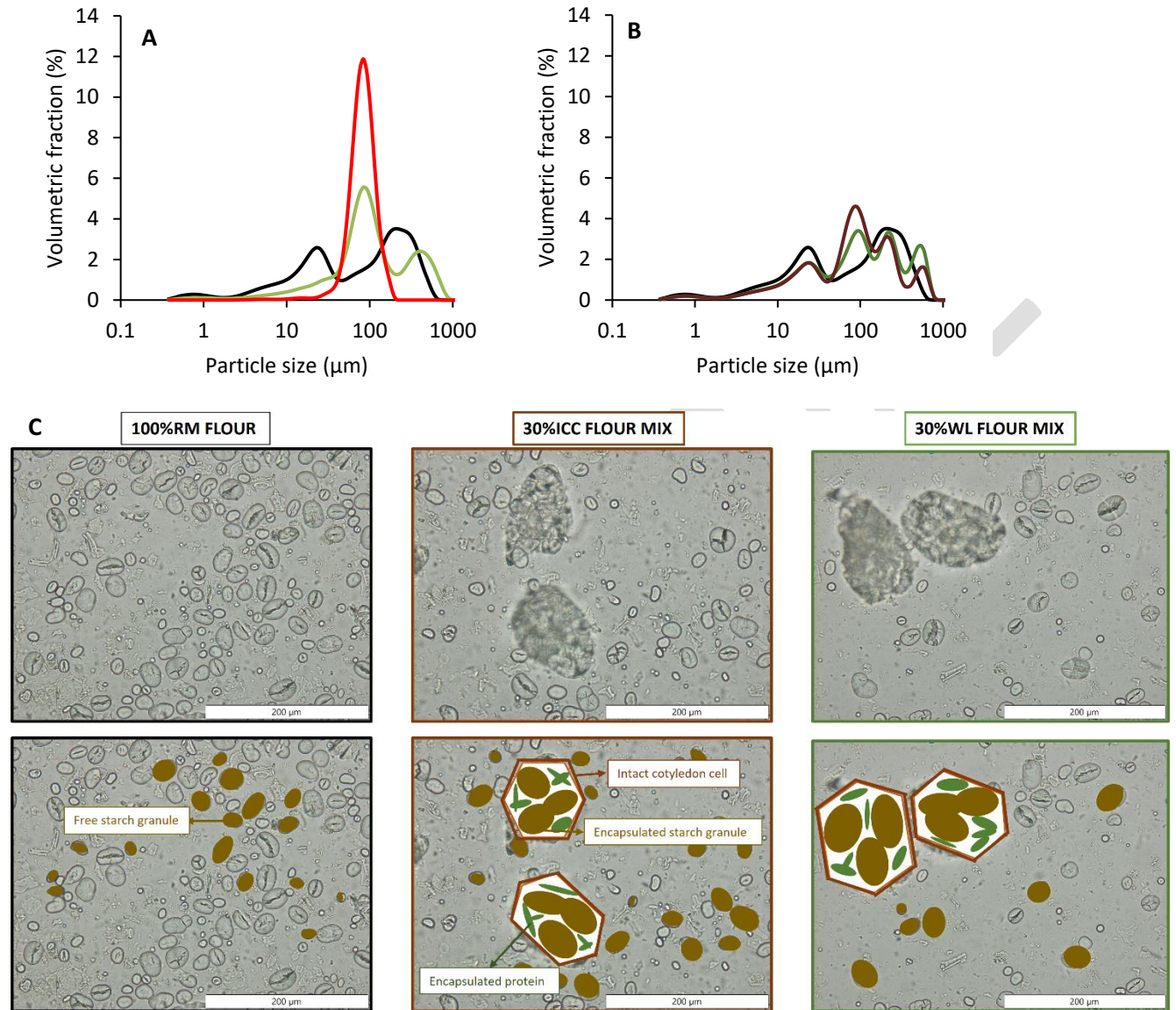


Figure S2: Particle size distributions (PSDs) and representative micrographs of lentil flours with different microstructures and their mixtures. A) PSDs of raw-milled (-), isolated cotyledon cell (ICC) (-), and whole precooked lentil (WL) (-) powders; B) PSDs of raw-milled (-) lentil flour, 30% ICC (-), and 30% WL (-) flour mixtures. C) representative micrographs of raw-milled flour (-), 30% ICC (-), and 30% WL (-) flour mixtures. (magnification 40x, scale bar 200  $\mu\text{m}$ ), the bottom row includes the same pictures, but with a schematical representation of the free and bio-encapsulated nutrients present in the flour mixes.

### Supplementary material 3

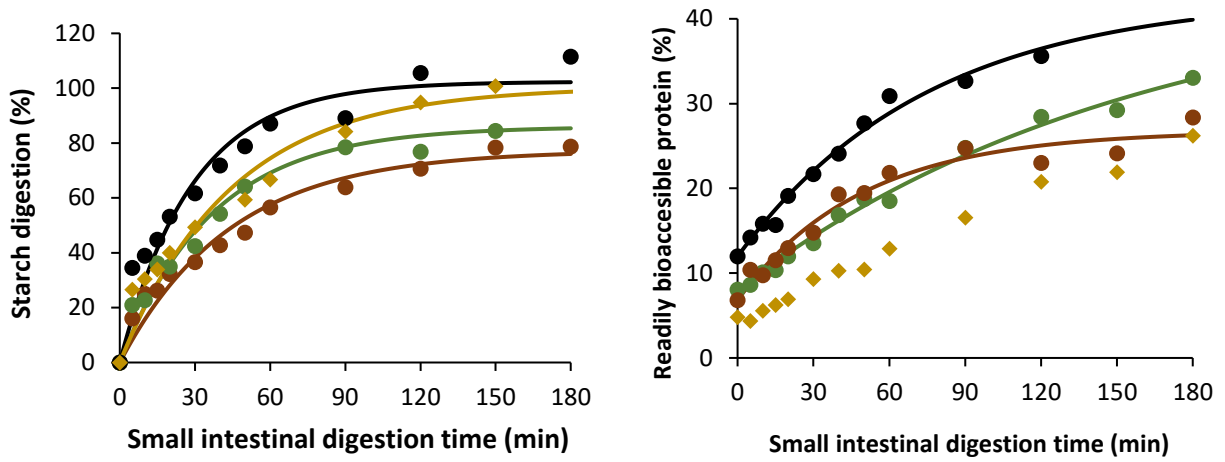


Figure S3: *In vitro* hydrolysis of starch and protein (in terms of readily bioaccessible protein, NH<sub>2</sub>TCA) of 100%RM (●), 30%ICC (●), and 30%WL (●) pastas cooked to their optimal cooking time (OCT), compared to a commercial 100% wheat-based spaghetti (◆) prepared according to the manufacturer's guidelines. Points are experimentally determined data. Lines represent the data modelled using the fractional conversion model, except for proteolysis of the wheat-based pasta, which did not follow this model.

CONFIDENTIAL

## Supplementary material 4

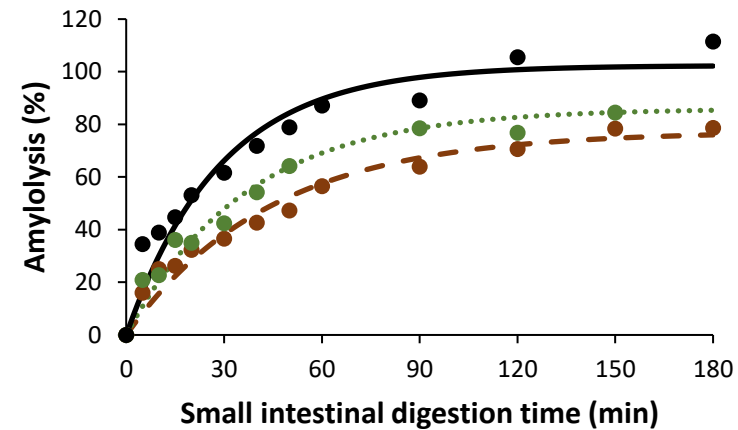
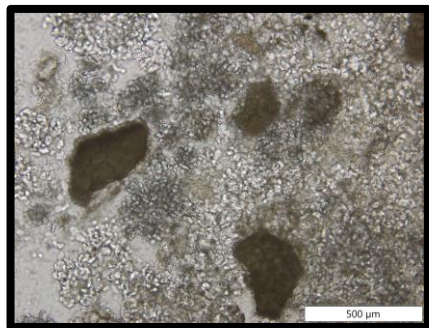
Table S4: Bioaccessible Ca, Mg, Fe, and Zn concentration (mg/100g cooked pasta, wet matter) and contribution to average daily requirement (ADR) of a reference portion of 100 g cooked pasta for 100%RM, 30%ICC, and 30%WL lentil spaghetti. Within one mineral type (column), different letters indicate statistical differences between the mean values (Tukey's range test,  $p < 0.5$ ).

Lentil pasta		Ca	Mg	Fe	Zn
100%RM	Bioaccessible mineral concentration (mg/100g cooked pasta, wet matter)	33.3 ± 1.9 <sup>a</sup>	46.6 ± 5.1 <sup>a</sup>	0.9 ± 0.2 <sup>a</sup>	0.9 ± 0.1 <sup>a</sup>
	Contribution to ADR (%) <sup>1</sup>	4.76	13.3	14.8	9.3
30%ICC	Bioaccessible mineral concentration (mg/100g cooked pasta, wet matter)	41.0 ± 9.8 <sup>a</sup>	34.0 ± 2.2 <sup>b</sup>	0.7 ± 0.1 <sup>a</sup>	0.5 ± 0.1 <sup>b</sup>
	Contribution to ADR (%) <sup>1</sup>	5.8	9.7	11.8	5.16
30%WL	Bioaccessible mineral concentration (mg/100g cooked pasta, wet matter)	31.4 ± 2.9 <sup>a</sup>	45.9 ± 4.6 <sup>a</sup>	0.7 ± 0.1 <sup>a</sup>	0.8 ± 0.1 <sup>a</sup>
	Contribution to ADR (%) <sup>1</sup>	4.5	13.1	12.2	7.8

<sup>1</sup>Contribution to the average daily requirement (ADR), based on average daily requirements of 700, 350, 6, and 10 mg/day for Ca, Mg, Fe, and Zn, respectively (EFSA, 2017).

100%RM: lentil pasta made of 100% raw-milled lentil flour; 30%ICC: lentil pasta made of 70% raw-milled flour and 30% isolated cotyledon cell powder; 30%WL: lentil pasta made of 70% raw-milled and 30% whole precooked lentil powder.

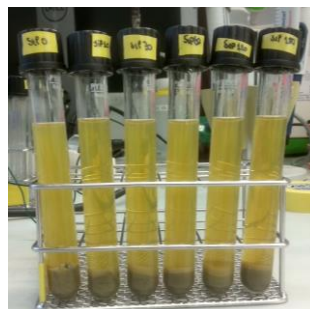
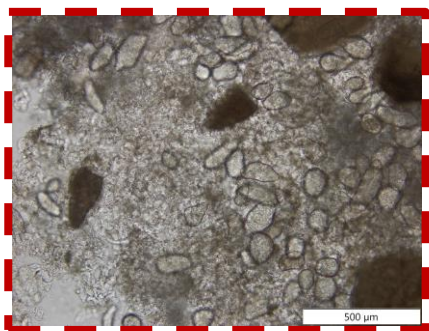
100% raw-milled flour



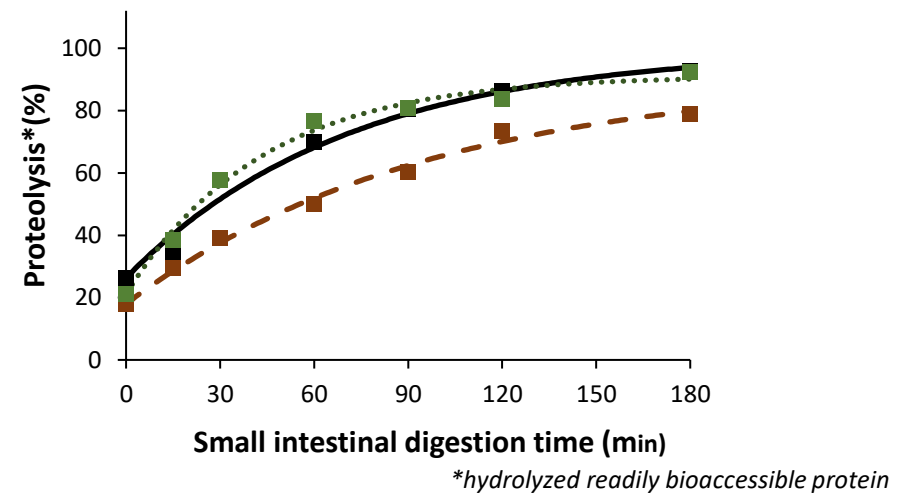
Lentil pasta



30% isolated cotyledon cell powder



In vitro digestion  
INFOGEST 2.0



30% whole precooked lentil powder

